Wind Tunnel Tests of Over-the-Wing Nacelles

J. Szodruch* and J. Kotschote†
MBB/Vereinigte Flugtechnische Werke GmbH, Bremen, Federal Republic of Germany

The aerodynamic performance of a typical transport aircraft semispan model with a stub-wing-mounted turbopowered simulator was experimentally investigated. The entire model was metric including the engine simulator. Various nacelle positions and jet velocity ratios were studied for two wing configurations. Results of force measurements show that there is an optimum nacelle position dependent on the wing configuration. Over-the-wing engines induce lift gains and higher maximum lift-drag ratios than conventionally mounted engines. Static pressure measurements on the wing indicate that mainly the upper side of the wing is influenced by over-the-wing engine simulation and that not only the jet but also the intake flow is important for interference effects.

Nomenclature

C = wing chord
C_D = drag coefficient
C_L = lift coefficient
C_M = pitching moment coefficient with respect to wing quarter chord line
c_p = pressure coefficient
D = fan exit diameter
M_∞ = freestream Mach number
OTW = over-the-wing
P_∞ = freestream static pressure
P_{tj} = total pressure in jet wake
Re = Reynolds number
TFN = through-flow nacelle
TPS = turbopowered simulator
UTW = under-the-wing
V_∞ = freestream velocity
V_j = jet velocity
$\bar{X}$ = axial distance measured from fan exit
X = longitudinal nacelle position with respect to wing leading edge
Y = spanwise distance measured from fuselage centerline
Z = vertical nacelle position with respect to wing chord plane
α = angle of attack, deg
Δ = difference of data
δ_{flap} = flap deflection angle, deg
δ_{slat} = slat deflection angle, deg

Introduction

IMPROVING the performance of an existing aircraft design is limited if major modifications are excluded. However, when special attention is given to nacelle/wing interference, performance gains may be achieved by placing the engines in over-the-wing positions. The aerodynamic advantages of these configurations compared to conventional designs have been demonstrated in some experimental and a few theoretical investigations. Over-the-wing engines were employed in early seaplanes[1] and also in various projects during World War II.[2] In the early 1960s the VFW 614 was designed and later built.[3,4] So far, it is the only aircraft flying with jet engines in over-the-wing positions. The concept was utilized primarily to improve takeoff and landing on undeveloped runways, to reduce trim, and to lower environmental effects such as noise. Further detailed studies revealed that improvements in lift and reductions in drag could also be achieved.[5,6] It was noted that the flow around the nacelle was of importance and that, furthermore, the jet strongly affects the flowfield. The airframe/engine interaction was studied in detail and revealed the interference between wing and jet.[7] An extensive investigation in the high-speed and transonic regime using a wing/body model with over-the-wing blown nacelles at various positions supported the low-speed results.[8]

Little attention was given to the nacelle support, which in the case of the VFW 614 was a pylon on the wing's upper surface. Based on the experience and knowledge gained with this aircraft, an advanced concept was designed where the nacelles were mounted on additional wings.[9] However, the additional wing increases the drag as compared to a normal pylon, but lift gains can be expected. In preliminary tests, the aerodynamic advantages of this concept were investigated and the results appeared promising.[10,11] Besides the aerodynamic, environmental, and handling improvements for aircraft with over-the-wing nacelles, possible disadvantages also have to be taken into consideration. The stub wing might impose

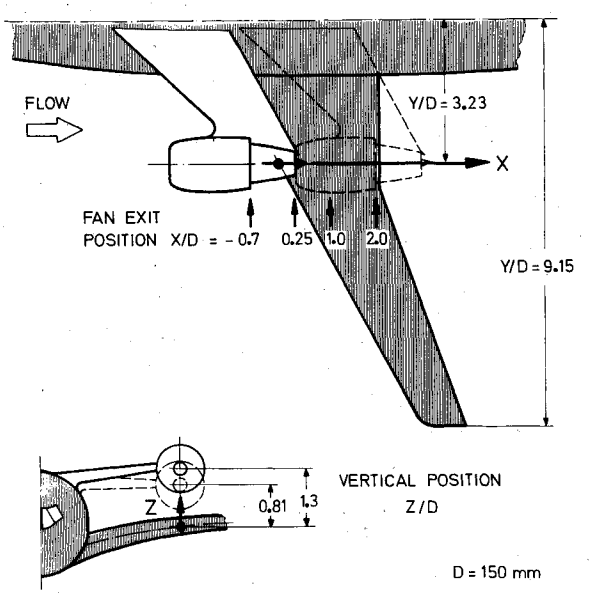

Fig. 1 Coordinate system and over-the-wing nacelle positions normalized to fan exit diameter *D*.

Received Nov. 15, 1982; presented as Paper 83-0538 at the AIAA 21st Aerospace Sciences Meeting, Reno, Nevada, Jan. 10-13, 1983; revision received Feb. 14, 1983.

*Research Scientist. Member AIAA.
†Research Engineer.

structural problems and certainly increases the weight of the aircraft substantially. Constructional problems may arise since fuel lines run through the pressurized cabin. Minor problems are seen in aggravated cabin acoustics and hampered passenger visibility.

In judging the aerodynamic effects of the interaction between the airframe and the engine, it is of extreme importance to simulate the propulsion system as realistically as possible. In all known over-the-wing engine investigations, flow-through nacelles, blown nacelles, or ejector simulators have been employed. These techniques are limited when compared with full-scale aircraft engines. The most recent and sophisticated concept is the turbopowered simulator (TPS) where correct operational conditions of pressure ratio, temperature, and mass flow of the fan jet and thrust of the gas generator nozzle can be achieved together with the geometric similarity of the nacelle. The intake mass flow in relation to the real engine is incorrect but can be corrected by a modified lip. The temperature of the primary nozzle jet is not simulated.[12,13]

In the present investigation, the importance of the interference effects made it necessary to employ the TPS as an engine simulator. In contrast to previous over-the-wing nacelle investigations, the stub-wing-mounted engine simulator was metric in the present study. The purpose of this paper is to investigate the effect of the advanced over-the-wing nacelle concept on the aerodynamic characteristics and to gain further insight into the flow mechanism.

Experimental

The experiments were conducted in the 2.1×2.1 m low-speed wind tunnel at freestream velocities of approximately 60 m/s, corresponding to a Mach number of 0.18 and a Reynolds number of 1.44×10^6. The baseline configuration was a semispan model, typical of a modern transport aircraft. Because of constructional problems, the stub wing presents a preliminary design and is not optimized for interference effects with the main wing. The entire model was metric including the stub wing and TPS.

Tests were performed with two wing configurations (cruise and takeoff), at jet/freestream velocity ratios ranging from windmilling ($V_j/V_\infty = 0.8$) to maximum takeoff ($V_j/V_\infty \approx 3.6$) and for two vertical and four longitudinal nacelle positions. The spanwise nacelle location remained in the same plane as on under-the-wing configurations. The position of the nacelle is defined in a coordinate system with the origin at the leading edge of the wing and is nondimensionalized with respect to fan exit diameter. The nacelle locations and the coordinate system are indicated in Fig. 1.

Essentially, interference effects will be present between the wing/body and the stub wing and nacelle; however, measurements were conducted only with wing/body, with wing/body and stub wing, and with the complete model (wing/body plus stub wing and nacelle). There might be some residual interference that cannot be accounted for; however, in analyzing influences the differences in these data will be used. The experiments concentrated mainly on obtaining force and static pressure measurements on the wing as well as on oil flow visualization.

Discussion

Interference between the airframe and the engine is of major concern. However, the detailed flow mechanism is often not understood well enough to predict the aerodynamic characteristics with confidence. This is true for under-the-wing nacelles and even more so for over-the-wing engine configurations. Therefore, it seems reasonable to start by analyzing preliminary wake flow surveys of the TPS jet and the static pressure measurements on the wing in an effort to understand the physics of the flow. The later discussion of the force measurements will indicate the improvements in aerodynamic efficiency.

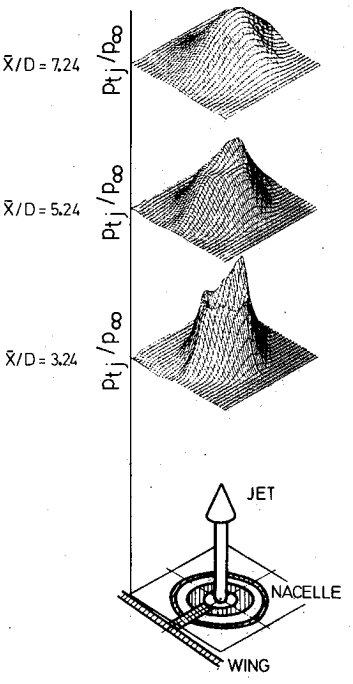

Fig. 2 Wake flow survey at different positions downstream of turbopowered engine simulator.

TPS Jet Flow

A rather limited number of publications provide TPS jet wake flow surveys,[14,15] and data for real engines are not available at all. The knowledge of classical free jets indicates that the characteristics of a jet are strongly dependent on freestream Mach number, nozzle pressure, jet temperature, flow angle at the jet exit, and the nozzle shape.[16] The TPS wake flow is further complicated by the interaction and mixing of the primary nozzle jet and fan jet. The total pressure distribution at three different locations downstream of the fan exit with the TPS in the under-the-wing position is shown in Fig. 2. The primary jet and fan jet can be distinguished near the fan exit, although major distortions from different sources result in a highly asymmetric flowfield. Unfortunately, this is the same region in which engine/wing interference is encountered. Further downstream the complex jet structure decays and, at more than seven fan diameters, the pressure distribution is very much like that of a classical free jet. This kind of wake flowfield occurs for other TPS jet velocities and for higher angles of attack. The TPS jet influence on the wing flowfield is complicated by the jet structure (i.e., asymmetric wake, temperature distribution, etc.) and so far it is impossible to predict accurately.

Some Aspects of Interference Flow Mechanism

In the following some details of the flow mechanism as affected by the influence of the stub wing, jet, and nacelle position will be discussed. Interference effects between the wing/body and stub wing without TPS were observed mainly near the fuselage, where the static pressure distribution on the upper side of the wing shows a strongly reduced suction peak at the leading edge because of the decreased local angle of attack. Downstream, the flow is accelerated again as a result of the changing geometry between the wing and stub wing. The magnitude of these changes depend on the angle of attack and the longitudinal and vertical positions of the stub wing.

Because of its size, the presence of the TPS results in distinct changes of the flowfield even without jet simulation (i.e., at conditions $V_j/V_\infty \leq 1.0$). In Fig. 3, the static pressure differences, jet-on and jet-off, on the upper surface of the wing are shown for three spanwise positions and an angle of attack of 5 deg. Operating the TPS with increasing velocity

ratios accelerates the flow over the first half of the wing chord. Even the plane of measurement near the fuselage (more than one fan diameter inboard of the nacelle) is affected, although only in the vicinity of the leading edge. This is observed at different longitudinal positions and is believed to be due not only to the jet but also to the intake flow. At spanwise stations close to the engine simulator, but slightly outboard, the flow is decelerated downstream of $X/C \approx 0.7$, that is, where the jet is presumed to be close to the upper surface. Overall, the jet/intake flow/wing interference is amplified by increasing velocity ratios and higher angles of attack.

Unfavorable interference effects develop when the nacelle is moved downstream to $X/D = 2.0$, where the intake and the fan exit lie near the leading edge and trailing edge, respectively. Figure 4 shows the pressure difference between jet-on and jet-off for this position. Acceleration of the flow around the leading edge is due to the intake flow. The extensive region of decelerated flow between the chord positions $X/C = 0.1$ and 0.8 is also believed to be an effect of the intake flow. It seems that the large blockage of the nacelle for the windmilling condition dominates, although the extension of the affected regime, spreading also in the spanwise direction, is unexpected and is not well understood. Further measurements show that the flow interferences are strongest for angles of attack of about 5 deg.

The foregoing discussion for over-the-wing nacelles indicates that the previously neglected inlet flow must be considered in addition to the flow contributions of the stub wing and the exhaust jet.

Interference Effects on Aerodynamic Force Coefficients

The effect of the stub wing will be discussed here only briefly. Depending on the angle of attack and the vertical and longitudinal positions of the nacelle, the stub wing increases lift. A rather severe increase in drag is observed because of the nonoptimum design of the stub wing. The reduction in maximum lift-drag ratio as a function of the longitudinal stub-wing position for two vertical stations is shown in Fig. 5.

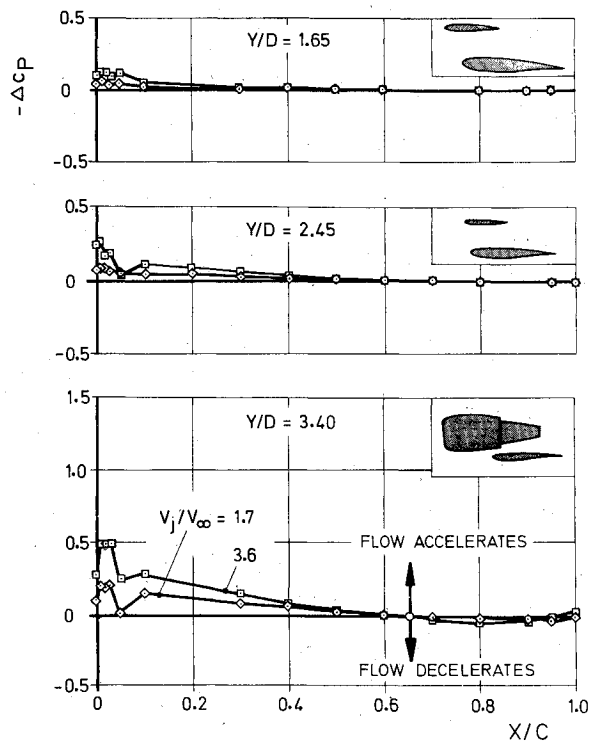

Fig. 3 Influence of jet and intake flow on static pressure distribution at $X/D = 0.25$ and $Z/D = 0.81$.

These results are compared with earlier VFW 614 experiments[10] where the stub wing was designed in more detail. Apart from the higher vertical distance for the VFW 614 stub wing, the comparison indicates the impact of optimization. It is interesting that some low-speed tests with canard configurations[17] gave evidence of reductions in maximum lift-drag ratio of only a few percent and that no considerable gains could be achieved with various geometric modifications. These results can be considered as an upper limit for the stub-wing design.

As already discussed, distinct flow changes are observed with the TPS. Operating the engine simulator at increasing velocity ratios accelerates the flow and produces additional lift. The lift gain due to the jet and intake flow as a function of angle of attack is shown in Fig. 6 and supports the earlier observations. Favorable interference from accelerated upperside flow is responsible for considerable lift gains at windmilling conditions (i.e., by just the presence of the nacelle). These data are strongly dependent on angle of attack. Even before the maximum lift is obtained, the flow is highly disturbed and partly separated. The jet/intake flow-induced lift gains are nearly uniform with angle of attack. The lift behavior, on the other hand, is also dependent on the nacelle position, since the pressure distributions have demonstrated strong interference effects between the nacelle and the wing for the far downstream TPS position ($X/D = 2.0$). At rather low angles of attack, flow separation occurs and lift losses are observed. Only high jet velocities seem to stabilize the flow.

Reubush[8] noted beneficial interference effects on wing/body drag when nacelles were present, while operation of the jet reduced this effect. In the present investigation with metric nacelles, interference effects of only the nacelles could not be accounted for; therefore, installing the engine simulator always results in a drag increase (Fig. 7). The

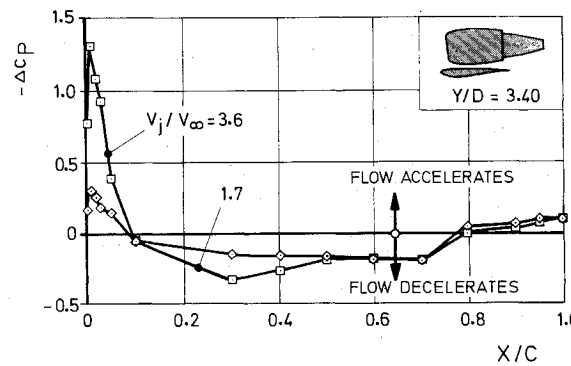

Fig. 4 Influence of jet and intake flow on static pressure distribution at $X/D = 2.0$ and $Z/D = 0.81$.

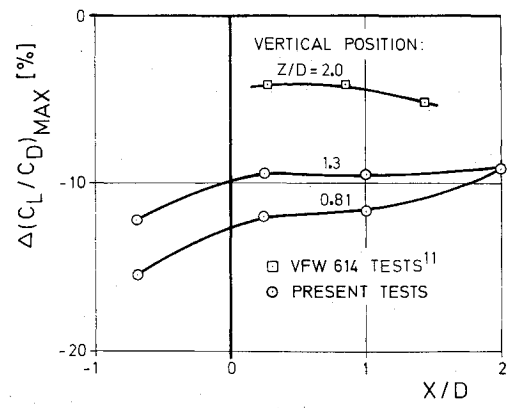

Fig. 5 Reduction in maximum lift-drag ratio due to stub wing at various longitudinal and vertical positions.

dominance of nacelle drag is also illustrated by the fact that at zero angle of attack the drag is nearly independent of longitudinal position, but strongly affected by the jet velocity. Furthermore, when the nacelle is moved downstream to a position just above the wing, the dependence on angle of attack is reduced and nearly uniform drag differences with α are observed. Operation of the TPS shows a drag reduction for lower jet velocities, while at higher V_j/V_∞, the beneficial jet interference tends to decrease, possibly due to jet impingement in the trailing-edge region of the wing.

When the drag difference with and without TPS is plotted vs longitudinal position (Fig. 8), an optimum position at about $X/D=0.25$ is noted. In Fig. 8a, for a cruise configuration, there is a tendency for the drag to increase with increasing nacelle height above the wing. On the other hand, these results are mainly due to interference between the jet/intake flow and wing, so drag reductions can be expected with further increases in vertical nacelle position. Obviously, the wing configuration has to be considered as well, since the optimum nacelle position in terms of drag is different for the Reubush[8] tests and the present experiment. This is also confirmed in Fig. 8b where the drag difference is plotted against longitudinal nacelle position for a takeoff configuration. The optimum vertical position is found at a higher value of $Z/D=1.3$. It is believed that for different configurations, the changing flowfield around the wing is responsible for the magnitude of the interference effects, and thus for different optimum nacelle positions as well.

A typical example of the pitching moment characteristics is shown in Fig. 9 for a nacelle position at $X/D=0.25$ and $Z/D=0.81$. The change in pitching moment is plotted with respect to wing/body results. In general, stub wings at the more upstream positions reduce stability. Operation of the TPS results in higher pitching moments because of induced lower static pressures near the leading edge. As already noted

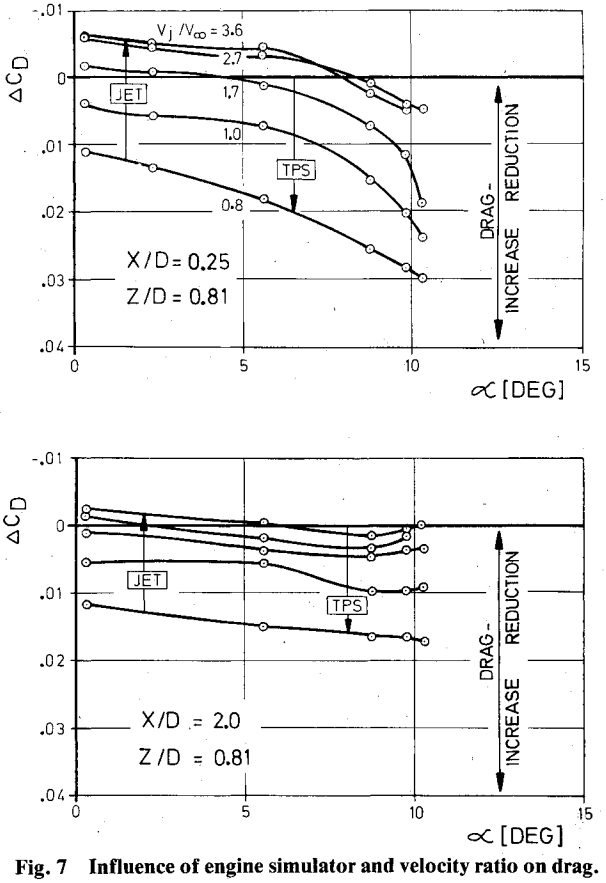

Fig. 7 Influence of engine simulator and velocity ratio on drag.

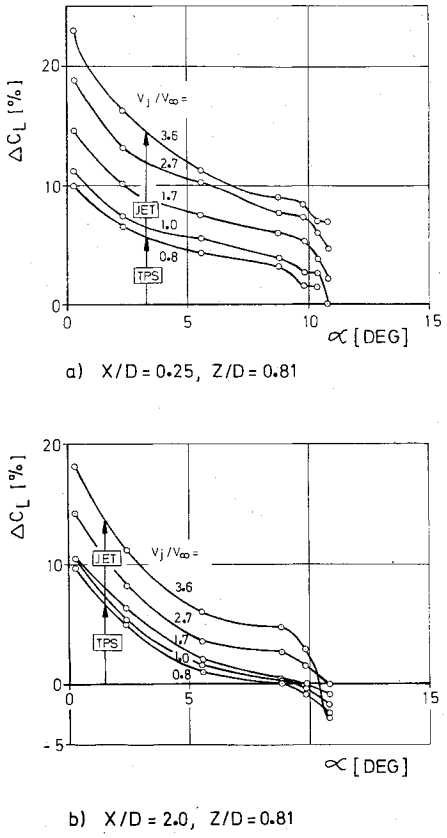

Fig. 6 Influence of engine simulator and velocity ratio on lift.

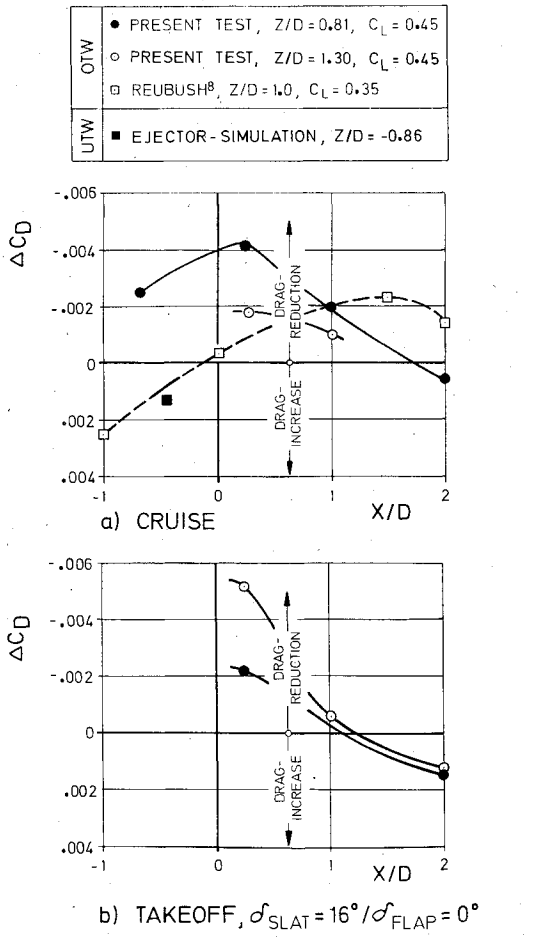

Fig. 8 Effect of longitudinal nacelle position on drag.

by Reubush,[8] major changes are observed between jet-on and jet-off. However, the pitching moment is rather insensitive to jet velocities. The slope $\partial C_M/\partial C_L$ is almost constant, with the level shifting toward lower stability when installing the stub wing and TPS. Although in general a tendency toward decreased stability is observed, the changes are rather small and would present no major design problem.

Finally, under-the-wing and over-the-wing engine arrangements are compared. The lift gain, always based on wing/body results, vs the angle of attack is plotted in Fig. 10 for a takeoff configuration at $V_j/V_\infty = 3.6$. In the under-the-wing data (unpublished results obtained with exactly the same baseline model and flow conditions), the influence of the pylon is included; however, it is believed that the pylon effects are small compared to the contribution of the nacelle. For the under-the-wing arrangement, lift losses occur, but are reduced at higher angles of attack. This is supported by pressure distributions over the wing where the upper surface is essentially affected. The flow-through nacelle data indicate that the effect of angle of attack on lift gain depends on the blockage effect of the nacelle rather than on the jet. For the over-the-wing engine position, these characteristics are reversed. At small angles of attack, beneficial effects caused by the stub wing (and even more by the TPS and jet/intake flow) lead to high lift gains. Increasing incidences tend to reduce these favorable effects. Especially at higher angles of attack, the flow on the upper surface is more sensitive to perturbations. Thus, engines above the wing cause more severe unfavorable effects than in under-the-wing positions. Furthermore, pressure distributions indicate beneficial interference with the lower-side flow when the engine position is under the wing, while the over-the-wing arrangement hardly affects the lower-side flow.

The change in maximum lift-drag ratio with respect to the wing/body including the stub wing is plotted against the vertical position of the nacelle in Fig. 11. Cruise and takeoff configurations are considered, with both over-the-wing and under-the-wing engine arrangements and longitudinal positions of $X/D = 0.25$ and -0.46, respectively. When the over-the-wing results for the cruise and takeoff configuration are compared, the slopes indicate the different flowfields around the wing, as discussed earlier. The absolute values of the lift-drag ratio have to be taken with care, since different velocity ratios influence the results. Direct comparison of over-the-wing and under-the-wing TPS data for the takeoff configuration proves the advantages of over-the-wing nacelle positions. Here, the difference in maximum lift-drag ratio is of the order of 6.5% with identical wing/body configurations and jet velocities. The data shown contain only the influence of the nacelle, jet, and intake flow, including the pylon in the case of the under-the-wing engine. For comparison and information, results with ejector simulation are included. However, the disadvantages of this kind of engine simulation when dealing with jet/wing interference effects are evident.

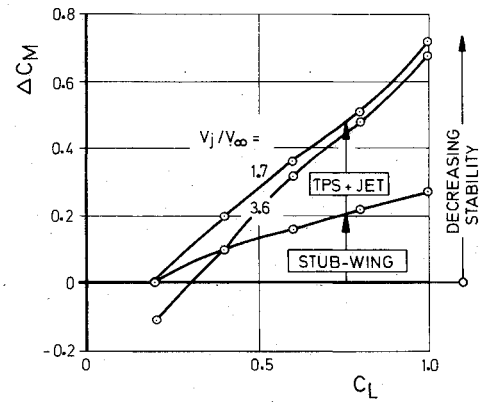

Fig. 9 Pitching moment characteristics at $X/D = 0.25$ and $Z/D = 0.81$.

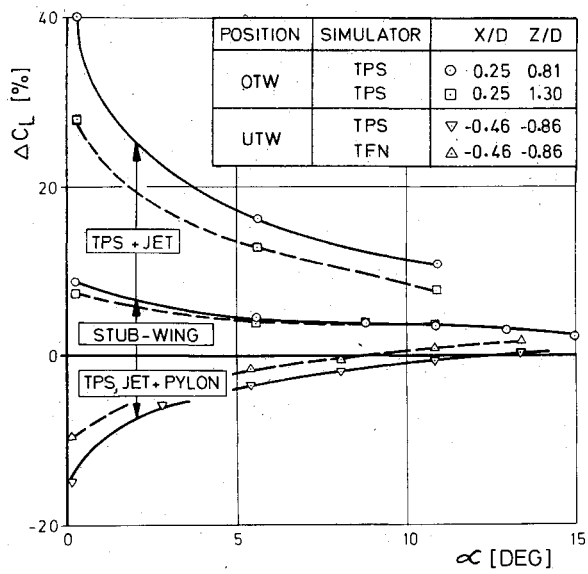

Fig. 10 Lift gain comparison between OTW and UTW nacelle position at $V_j/V_\infty = 3.6$.

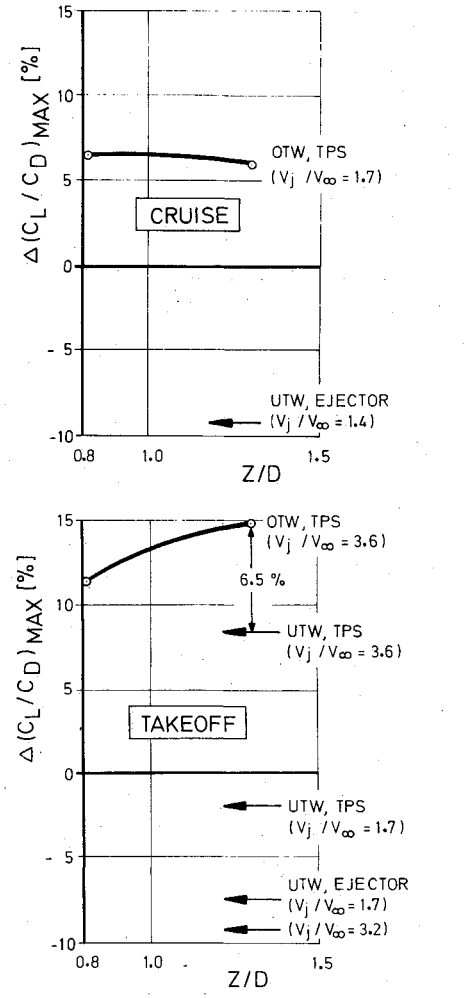

Fig. 11 Maximum lift-drag ratio for OTW and UTW nacelle position employing different engine simulators and velocity ratios.

Conclusions

An advanced over-the-wing nacelle concept has been experimentally investigated to study the interference effect of powered nacelles, stub wing, and wing/body on the aerodynamic characteristics and to gain some insight into the flow mechanism. Static pressure distributions on the wing revealed that only the upper surface is influenced by the nacelle and jet, as long as the fan exit is close to the upper surface or well downstream of the wing leading edge, e.g., above the trailing edge. The contribution of the turbopowered engine simulator to the lift is caused by increased suction over only the upstream half of the wing chord. Not only the jet, but also the intake flow, neglected in previous investigations, has to be considered for interference effects.

The analysis of the aerodynamic characteristics indicated lift gains but a reduction in maximum lift-drag ratio due to the stub wing. However, substantial lift gains and drag reductions can be achieved by operating the engine simulator with increasing velocity ratios. Favorable interference effects occur for certain longitudinal engine locations. Vertical nacelle positions are less important. Optimum nacelle positions are dependent on the wing configurations. With identical wing/body configurations and TPS velocity ratios, the over-the-wing engine yields higher maximum lift-drag ratios than under-the-wing arrangements.

Acknowledgment

This work was supported by the German Ministry of Research and Technology (BMFT).

References

[1] "DO X 1929," Dornier GmbH, Friedrichshafen, FRG, Jan. 1979.

[2] Kens, K. and Nowarra, H.J., *Die deutschen Flugzeuge 1933-1945,* J.F. Lehmann, München, FRG, 1961.

[3] "Passagier- und Frachtflugzeug VFW 614," VFW, Bremen, FRG, Tech. Rept. 11-64, 1964.

[4] Barche, J., "Tragflügelentwurf am Beispiel des Verkehrsflugzeuges VFW 614," *Zeitschrift für Flugwissenschaften,* Vol. 22, April 1974, pp. 101-115.

[5] Putnam, L.E., "An Analytical Study of the Effects of Jets Located More Than One Jet Diameter above a Wing at Subsonic Speeds," NASA TN D-7754, 1974.

[6] Fischer, F. and Hilbig, R., "Gegenseitige Beeinflussung von Zellen- und Triebwerkströmung," BMFT, Bremen, FRG, Rept. Nr. IB 3-8391-LFF6, 1973.

[7] Krenz, G. and Ewald, B., "Airframe-Engine Interaction for Engine Configurations Mounted above the Wing," AGARD CP 150, 1975, Paper 26.

[8] Reubush, D.E., "Effect of Over-the-Wing Nacelles on Wing-Body Aerodynamics," *Journal of Aircraft,* Vol. 16, June 1979, pp. 359-365.

[9] Krenz, G., "Aerodynamische Auslegung und Flugerprobung der VFW 614," Paper DGLR 76-208, 1976.

[10] Fischer, F., Franz, H.P., John, R., and Kaszemeik, K., "Auftriebs- und Vortriebskonzepte bei zukünftigen Transportern," Rü IV 1, Bremen, FRG, Rept. T/R 412/70003/72401, 1977.

[11] Fischer, F., Franz, H.P., Brix, W., and Kaszemeik, K., "Auftriebs- und Vortriebskonzepte bei zukünftigen Transportern," Rü IV 1, Bremen, FRG, Rept. T/R 421/80006/82405, 1978.

[12] Burgsmüller, W., "Grundlagen zur Triebwerksimulation mittels TPS im Windkanal," VFW, Bremen, FRG, Rept. Ef 915, ZKP-IFAS-Rept. 5, 1980.

[13] Ewald B. and Smyth, R., "The Role and Implementation of Different Nacelle/Engine Simulation Concepts for Wind-Tunnel Testing in Research and Development Work on Transport Aircraft," AGARD CP 301, 1982, Paper 22.

[14] Burgsmüller, W., "Results of 1st Phase Windtunnel Tests with TPS on A 300-halfmodel 123.3 in the VFW-LST", Deutsche Airbus GmbH, Bremen, FRG, Doc-Nr. 00II-X001.77088, VFW Rept. KB-Ef 1025, 1981.

[15] Ewald, B. and Burgsmüller, W., "Experimental Investigation of Transport Aircraft Low Speed Interference Effects and Flight Test Correlation," AGARD Ground/Flight Test Techniques and Correlation, Cesme, Turkey, Oct. 1982.

[16] Zacharias, A., "Experimentelle und theoretische Untersuchungen über die Wechselwirkung zwischen Triebwerksstrahl und dem umgebenden Strömungsfeld," Dissertation, Technical University Braunschweig, FRG, 1981.

[17] Kühn, A., "Untersuchung zu Canard-Einflüssen am Airbus A 300-B4," DFVLR, Göttingen, FRG, Rept. IB 157-80 C 09, 1980.